International Journal for Multidisciplinary Research (IJFMR)
E-ISSN: 2582-2160 ● Website: www.ijfmr.com ● Email: editor@ijfmr.com

Mathematical Modelling of Non-Newtonian Flow of Mandarin Juice Over a Moving Permeable Sheet with Slip and Heat Generation

Dr. Ruhul Kuddus Ahmed

Department of Mathematics, Bilasipara College, Bilasipara, Dhubri, Assam, India.

Abstract

The non-Newtonian flow of mandarin juice over a moving permeable sheet with slip condition and heat generation is investigated. The shear-thinning nature of mandarin juice under certain prescribed conditions is mathematically studied with the help of the Power-Law fluid model. The fluid flow motion of mandarin juice is governed by a set of partial differential equations along with relevant boundary conditions. The appropriate similarity variables are utilized to obtain the resulting governing equations. The graphical representation of velocity and temperature profiles are obtained by solving the governing equations by employing finite difference method-based MATLAB solver 'bvp4c'. The impact of velocity slip parameter, heat generation or absorption parameter, non-Newtonian flow index, and Eckert number are analyzed from graphs, and conclusions are drawn from a physical viewpoint. The local values of skin friction and Nusselt number are also tabulated to notice the effects of involved flow parameters.

Keywords: Mandarin Juice, Power-law fluid, Slip velocity, Heat generation, Eckert number.

1. Introduction

Food is one of the most important things for living beings. It provides energy, stimulate growth and helps to fight against diseases. Because of the growing interest in human health and diet around the world, vegetables and fruits are in demand due to their nutritional value. Thus, the development of products and industrial fruit and vegetable processing has greatly increased. The design of the transportation system for fluid food products is heavily influenced by the nature and description of the product's flow characteristics. The essential basis of mass transmission is flow characteristics. In reality, the fluid flow characteristics affect the product's overall qualities. For the design of products, the assessment of manufacturing procedures, and the formulation of packaging and storage plans, it is crucial to examine the flow characteristics of fluid fruit and vegetable products exhibiting non-Newtonian nature and how they behave when flowing through circular pipe, plate, and stretching sheet.

The mandarin orange is a tiny citrus fruit that grows on citrus trees. It is believed to be originated from ancient China and are grown in countries like Japan, Vietnam, India, and in many more countries. It contains rich variety of nutrients like calories, protein, vitamin, fat, fiber, magnesium and also contains antioxidant. Health benefits include boosting immune system, prevent aging, provide heart-healthy fiber, help to maintain or lose weight, reduce kidney stone risk.

A comprehensive assessment of the latest researches on the rheological characteristics of products made from fruit and vegetables has been presented by Diamante and Umemoto [1]. Abdulagatov et al. [2]

investigated at how temperature, pressure, and concentration influenced fruit juice viscosity. The rheologic properties of concentrated mandarin juice at lower temperature was examined by Falguera et al [3]. Vandresen *et al.* [4] illustrated the impact of temperature on the rheological characteristics of carrot juices. The temperature and concentration effect on the orange juice concentrate flow demonstrated by Vitali *et al.* [5]. Mahmoud [6] investigated the influence of slip velocity on the non-Newtonian flow past a moving porous surface with heat generation obeying power law fluid model. The critical examination of rheological properties of fluids from clarified passion fruit carried out by Ibarz *et al.* [7]. The master-curve modelling of the rheological properties of concentrates of pummelo juice was established by Chin et al. [8]. For industrial applications, Goula and Adamopoulos [9] established the rheological models of kiwifruit juice. The rheological properties of tomato juice at steady state and time dependent modelling have been carried out by Augusto *et al.* [10]. Research works on fluid flow using power law constitutive model have been done by Acrivoset al. [11], Schowalter [12], Lee and Ames [13], Anderssonet al. [14]and Sarithaet al. [15]. Besides going through these research papers, I have gone through some fluid mechanics books [16-18].

The objectives of this study are as follows:

- Mathematical modelling of mandarin juice for processing applications.
- Examine the impacts of the various solution-related physical flow factors.
- Investigate the flow patterns for different flow index values along with other flow guided parameters.
- Study the heat transition of non-Newtonian flow of mandarin juice.
- Interpret results from graphs and tables to get physical insight of the solved problems.

2. Mathematical Formulation

The following assumptions are considered to examine the flow and heat transition of mandarin juice past a continuously moving porous surface by Power-law fluid model:

1. The flow is incompressible, steady and laminar.
2. The two-dimensional boundary layer flow.
3. The constant velocity U is taken along x-direction.

The physical sketch of flow model is displayed in Fig. 2.1.

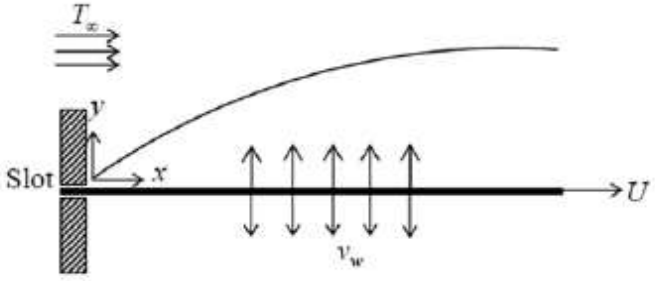

Fig. 2.1

The non-Newtonian shear-thinning nature of mandarin juice flow under certain prescribed conditions in addition to the results of heat generation and energy loss is guided by the following equations:

$$u_x + v_y = 0 \tag{2.1}$$

$$uu_x + vu_y = \frac{\mu}{\rho}\left(|u_y|^{n-1}u_y\right)_y \tag{2.2}$$

$$uT_x + vT_y = \alpha T_{yy} + \frac{\mu}{\rho c_p}\left|u_y\right|^{n+1} + \frac{Q_0}{\rho c_p}(T - T_\infty) \qquad (2.3)$$

Boundary conditions imposed at the boundary are:

$$At\ y = 0: u = U + \lambda\left(\left|u_y\right|^{n-1}u_y\right), v = -v_w,\ T = T_W \qquad (2.4)$$

$$As\ y \to \infty:\ u \to 0,\ T \to T_\infty \qquad (2.5)$$

where,

u- velocity along x-axis
v- velocity along y-axis
ρ-fluid density
μ-coefficient of viscosity
α-thermal diffusivity
c_p- specific heat at constant pressure
T_W - temperature of the plate
T_∞- temperature far away from plate
v_w - constant normal wall velocity
λ- slip velocity coefficient
n- flow index

Following similarity variables are introduced to get the dimensionless form of the self-similar governing equations:

$$\Psi = \sqrt[n+1]{\nu x U^{2n-1}}\, f(\eta), \eta = \sqrt[n+1]{\frac{U^{2-n}}{\nu x}}\, y, T = T_\infty + (T_w - T_\infty)\theta(\eta) \qquad (2.6)$$

with stream functions $u = \Psi_y$ and $v = -\Psi_x$.

Using these transformations, the governing equations (2.2) and (2.3) are reduced as follows:

$$n(n+1)f'''(f'')^{n-1} + ff'' = 0 \qquad (2.7)$$

$$\theta'' + \frac{Pr}{n+1}f\theta' + PrEc|f''|^{n+1} + \gamma Pr\theta = 0 \qquad (2.8)$$

where,

Ψ –dimensionless stream function
θ – dimensionless temperature
η – similarity variables
Pr- Prandtl number
Ec- Eckert number
γ – heat generation parameter

The relevant boundary conditions (2.4) and (2.5) are transformed as

$$At\ \eta = 0: f = f_w, f' = 1 + \lambda(f''|f''|^{n-1}),\quad \theta = 1 \qquad (2.9)$$

$$As\ \eta \to \infty: f' = 0, \theta \to 0 \qquad (2.10)$$

where,

f_w - suction/injection parameter and λ – slip parameter.

3. Method of Solution

The Matlab solver 'bvp4c' is employed to evaluate a system of linear or non-linear BVP. This approach is distinct from the shooting approach and is algorithm-based. It can efficiently calculate the approximation of y(x) for every x in [a,b] while taking boundary conditions into account at each stage. With this approach, the boundary conditions at infinity are swapped out for those at a position that reasonably solves the presented issue. To apply finite difference method-based solver 'bvp4c', the resultant governing equations (2.7) and (2.8) are transformed as follows:

$$f = y_1, f' = y_2,\ f'' = y_3, \theta = y_4, \theta' = y_5 \qquad (3.1)$$

$$y_1' = y_2,\ y_2' = y_3,\quad y_4' = y_5 \qquad (3.2)$$

$$y_3' = \frac{1}{n(n+1)}(y_1 y_3 |y_3|^{1-n}) \quad (3.3)$$

$$y_5' = -\gamma Pr y_4 - \frac{Pr}{n+1}(y_1 y_5) - PrEc|y_3|^{n-1} \quad (3.4)$$

Boundary conditions are transformed as follows:

$$y_1(0) = f_w, y_2(0) = 1 + \lambda(y_3(0)|y_3(0)|^{n-1}),\ y_4(0) = 1 \quad (3.5)$$

$$y_2(\infty) = 0, \qquad y_4(\infty) = 0 \quad (3.6)$$

The numerical computation is carried out by the solver 'bvp4c' with the help of the above transformed results.

4. Results and discussion

The effect of involved flow parameters viz. suction, slip, heat generation, Prandtl number and Eckert number on the dimensionless velocity profile $f'(\eta)$ and temperature profile $(\theta(\eta))$ of mandarin juice flow over a moving permeable sheet for three distinct values of flow index n = 0.699, n=0.721 and n = 0.746 exhibiting pseudo-plastic nature of fluid are presented in Figs. 4(a)-4(n). Local skin-friction $\left(\frac{Cf_x Re_x^{\frac{1}{n+1}}}{2} = -f''(0)|f''(0)|^{n-1}\right)$ and Nusselt number $\left(\frac{NU_x}{Re_x^{\frac{1}{n+1}}} = -\theta'(0)\right)$ are tabulated in Table 4.2 and 4.3

Table 4.1: Rheological parameters of mandarin juice

Product	C °Brix	Temp., °C	k, Pa.s^n	n
Mandarin Juice	63.3	6	3.9700	0.699
		-3	3.9800	0.721
		-9	6.9100	0.746

The fluid velocity curves $f'(\eta)$ diminishes with the growth of flow index parameters as seen in Fig. 4.1. Fig. 4.2 (a)-(c) display the response of suction parameter (f_w) on $f'(\eta)$ for three different values of flow index n. The suction parameter $(f_w > 0)$ improves fluid motion close to the boundary layer region, allowing the flow to pierce the fluid more deeply. The slip parameter's (λ) impact on the dimensionless velocity $f'(\eta)$ is seen in Fig. 4.3 (a)-(c). As the slip parameter rises, it can be seen that the dimensionless velocity falls at the surface but grows at greater distances.

It is noticed from Fig. 4.4, that the temperature profile $\theta(\eta)$ enhances with growing values of flow index parameters. Fig.4.5 (a)-(c) displays the response of suction parameter $(f_w > 0)$ on temperature profile $\theta(\eta)$. The fluid temperature reduces with the growth of suction parameter. Thus, it can be interpreted physically that greater suction causes the plate to cool more quickly, which is crucial in many technical applications. The slip parameter's (λ) impact on the temperature profiles is seen in Fig. 4.6 (a)-(c). As the slip parameter rises, temperature rises in the boundary layer region.

The impact of the heat generation parameter (> 0) on temperature profile is depicted in Figs. 4.7 (a)-(c). The heat generation causes the entire boundary layer's temperature to rise when $\gamma > 0$. It is also importantly noted that, when there is sufficient heat generation, the fluid layer close to the wall instead of at the wall itself experiences the highest fluid temperature. Physically, when heat generating effects are present, the fluid temperature has a tendency to rise, thickening the thermal boundary layer.

The influence of Prandtl number Pr on the dimensionless temperature profiles are presented in Fig. 4.8 (a)-(c). It is observed that when Pr rises, the dimensionless temperature falls. Physically, for three distinct values of the flow index parameters, raising Pr results in a reduction in the thickness of the thermal boundary layer.

Fig. 4.9 (a)-(c) demonstrates the non-dimensional temperature distribution for three distinct values of the Eckert number Ec in the boundary layer domain. It is evident that as Ec rises, the dimensionless temperature rises as well. As anticipated, a greater value of Ec is seen to cause a more noticeable growth of fluid temperature caused by viscous heating The reason for this is that decreasing the Eckert number cools the wall, which subsequently conducts heat to the fluid and raises its temperature.

Table 4.2 shows the impact of the slip parameter λ and the suction parameter f_w on the local skin-friction coefficient. This table shows that with rising values of the flow index parameters, the growth of the slip parameter λ results in a drop in the localized coefficient of skin-friction while the growth of the suction parameter f_w boosts the same factor.

Table 4.3 demonstrates the impact of the suction parameter f_w , slip parameter λ, heat parameter γ,Prandtl number Pr and Eckert number Ec on the Nusselt number for three different values of the flow index n. It is observed that as the suction parameter grows, the local Nusselt number rises while the opposite effect is produced by the slip parameter. A drop in the local Nusselt number results from an increase in heat generation. This is due to the fact that the heat generation process raises fluid temperature close to the surface, which causes a decrease in the temperature gradient at the surface and a reduction in heat transfer at the plate. Also, the local Nusselt number enhances when the Prandtl number Pr reduces. This happens because a fluid with a higher Pr has a higher heat capacity, which enhances heat transfer. However, as Eckert number Ec enhanced, the local Nusselt number diminished. The fact that the wall temperature gradient is negative for all parameter values indicates that heat is physically moving from the surface to the surrounding fluid.

Fig. 4.1 $f'(\eta)$ against η for variation of flow index n

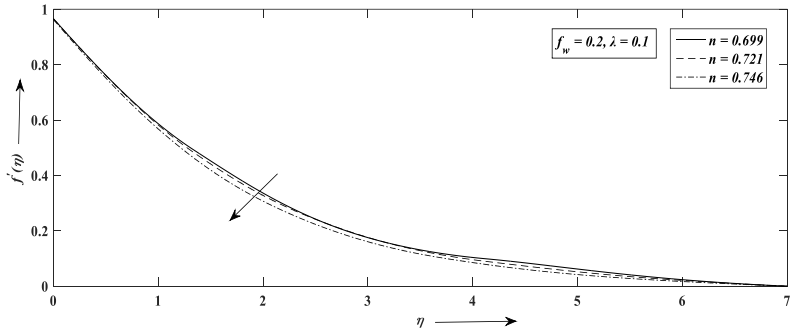

Fig. 4.2 (a) $f'(\eta)$ against η for variation of $f_w(> 0)$ for $n = 0.699$

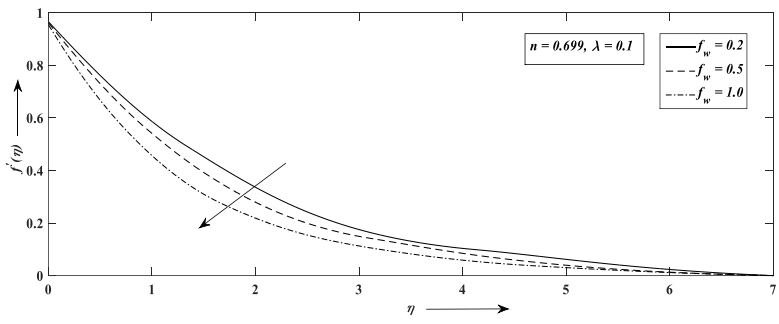

Fig. 4.2 (b) $f'(\eta)$ against η for variation of $f_w(>0)$ for $n = 0.721$

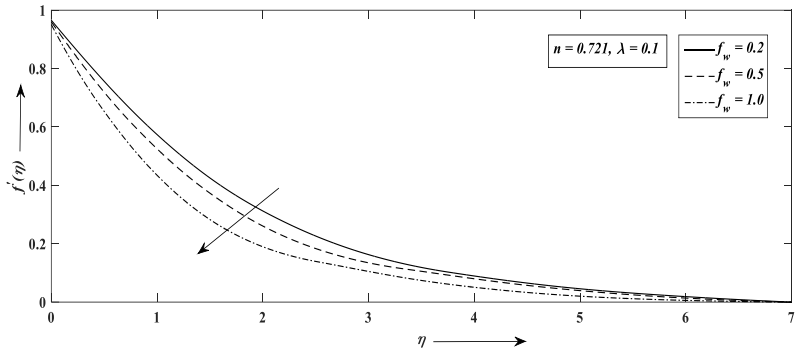

Fig. 4.2 (c) $f'(\eta)$ against η for variation of $f_w(>0)$ for $n = 0.746$

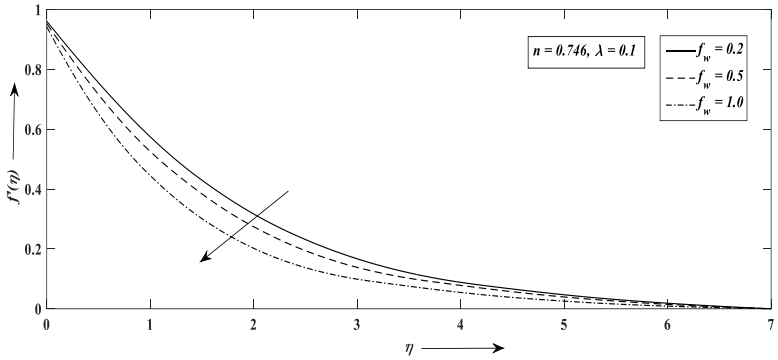

Fig. 4.3 (a) $f'(\eta)$ against η for variation of λ for $n = 0.699$

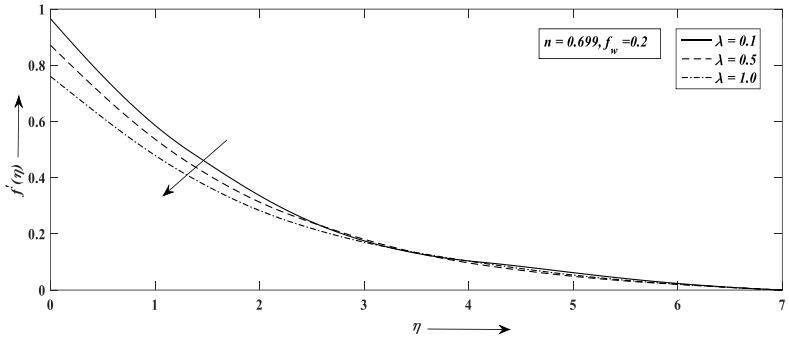

Fig. 4.3 (b) $f'(\eta)$ against η for variation of λ for $n = 0.721$

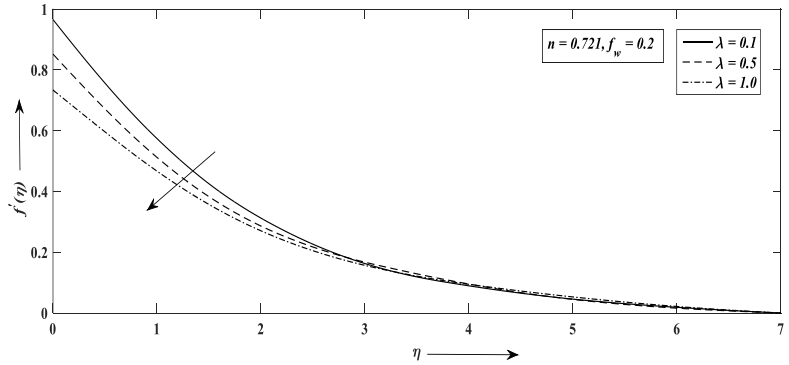

Fig. 4.3 (c) $f'(\eta)$ against η for variation of λ for $n = 0.746$

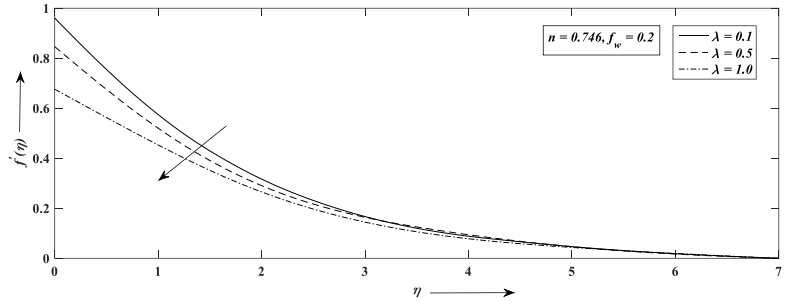

Fig. 4.4 $\theta(\eta)$ against η for variation of flow index n

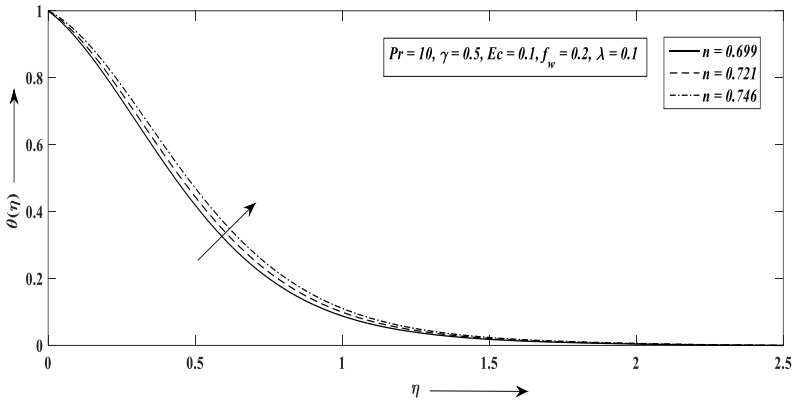

Fig. 4.5 (a) $\theta(\eta)$ against η for variation of $f_w(>0)$ for $n = 0.699$

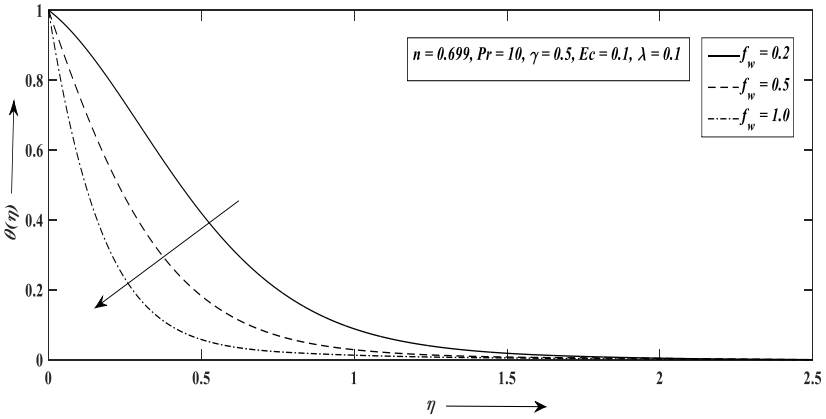

Fig. 4.5 (b) $\theta(\eta)$ against η for variation of $f_w(>0)$ for $n = 0.721$

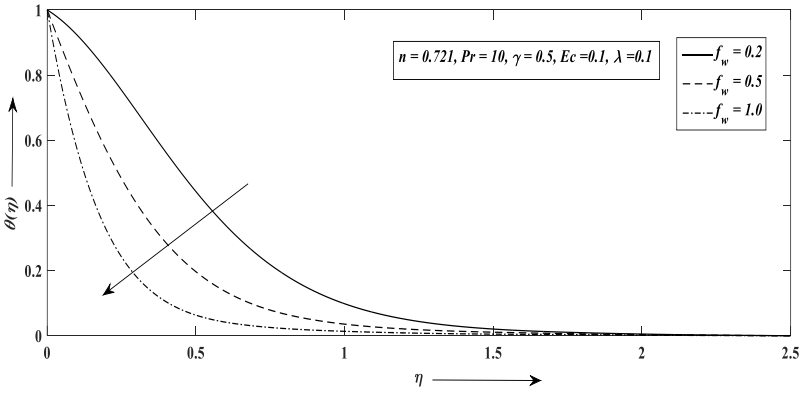

Fig. 4.5 (c) $\theta(\eta)$ against η for variation of $f_w(>0)$ for $n = 0.746$

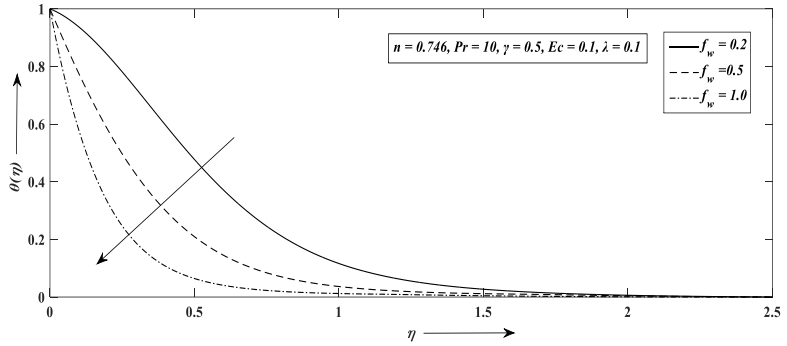

Fig. 4.6 (a) $\theta(\eta)$ against η for variation of λ for $n = 0.699$

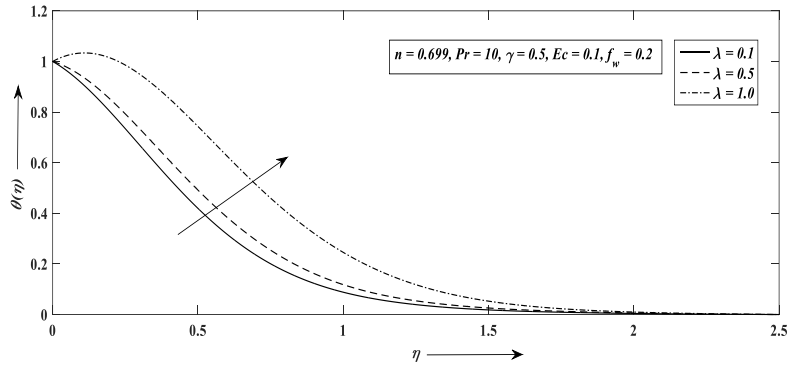

Fig. 4.6 (b) $\theta(\eta)$ against η for variation of λ for $n = 0.721$

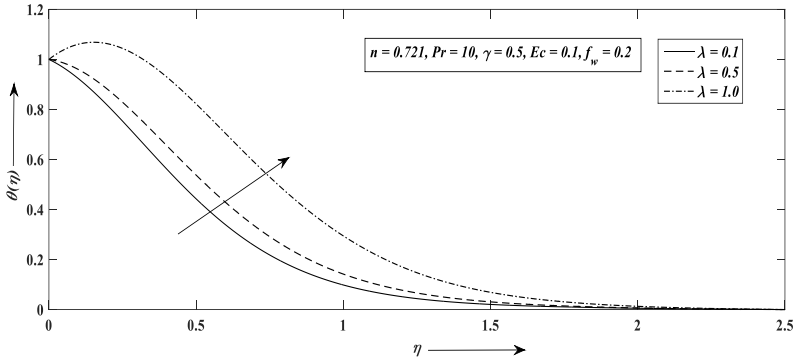

Fig. 4.6 (c) $\theta(\eta)$ against η for variation of λ for $n = 0.746$

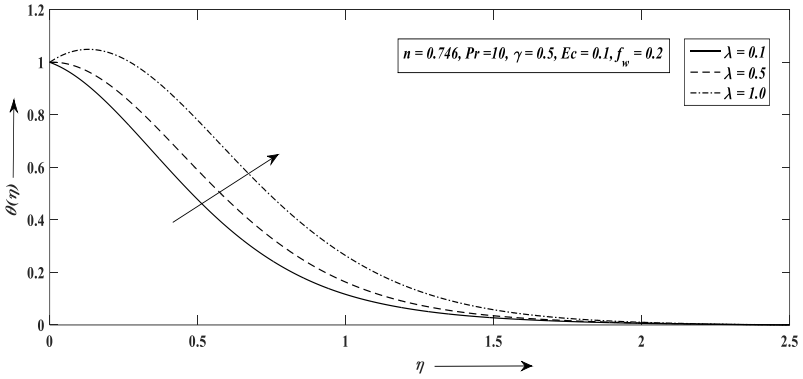

Fig. 4.7 (a) $\theta(\eta)$ against η for variation of γ for $n = 0.699$

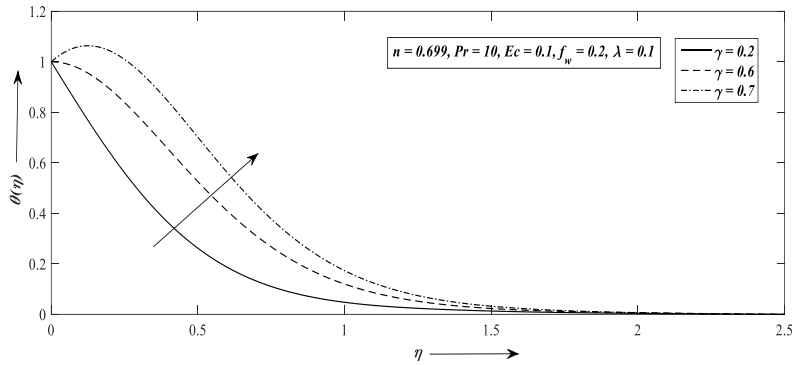

Fig. 4.7 (b) $\theta(\eta)$ against η for variation of γ for $n = 0.721$

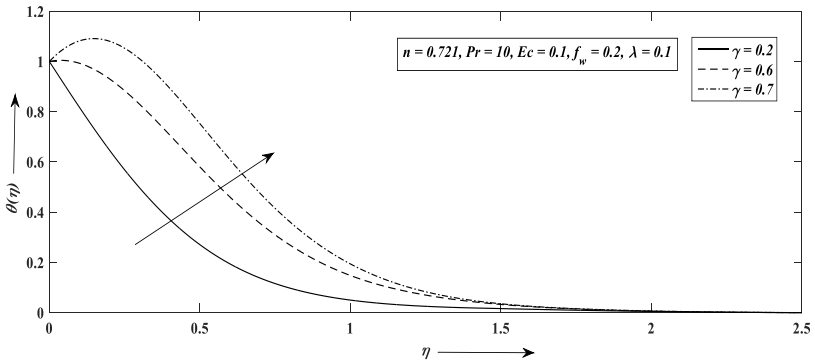

Fig. 4.7 (c) $\theta(\eta)$ against η for variation of γ for $n = 0.746$

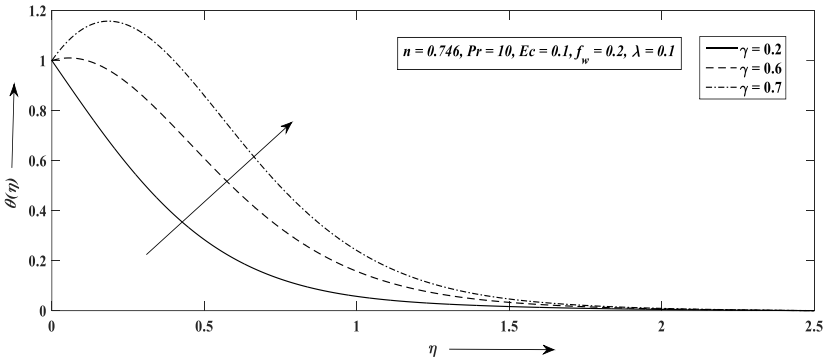

Fig. 4.8 (a) $\theta(\eta)$ against η for variation of Pr for $n = 0.699$

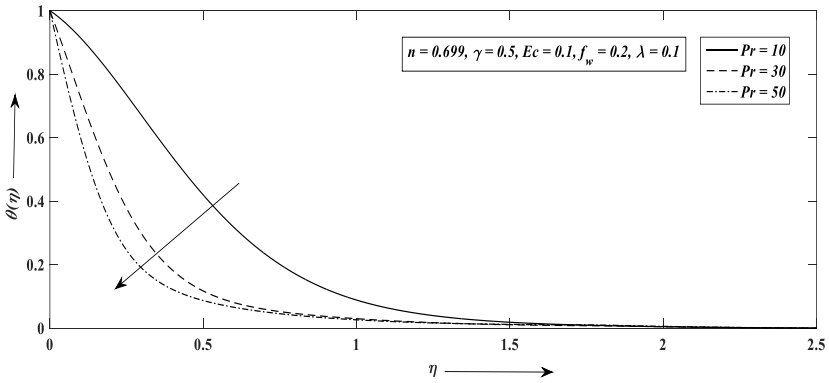

Fig. 4.8 (b) $\theta(\eta)$ against η for variation of Pr for $n = 0.721$

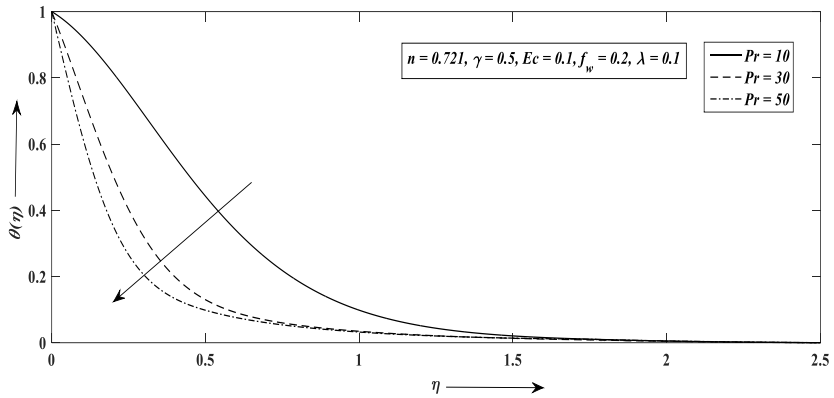

Fig. 4.8 (c) $\theta(\eta)$ against η for variation of Pr for $n = 0.746$

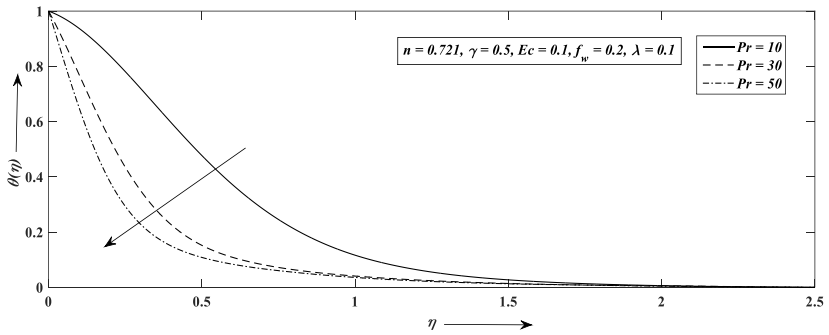

Fig. 4.9 (a) $\theta(\eta)$ against η for variation of Ec for $n = 0.699$

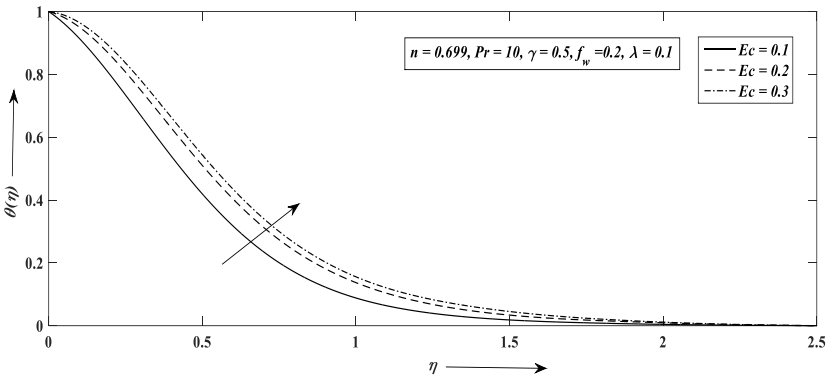

Fig. 4.9 (b) $\theta(\eta)$ against η for variation of Ec for $n = 0.721$

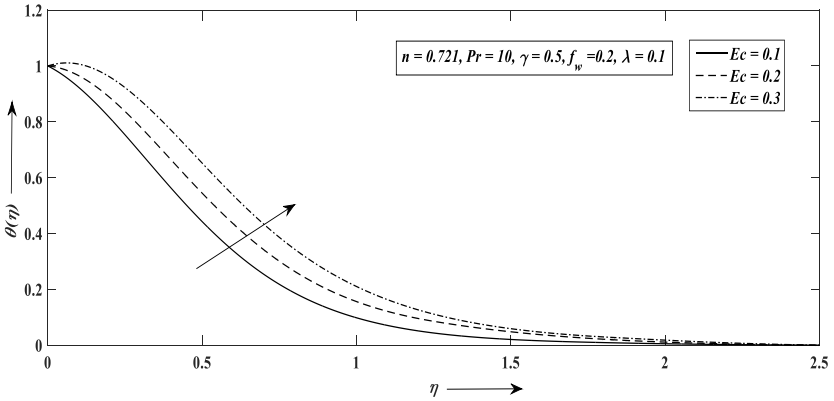

Fig. 4.9 (c) $\theta(\eta)$ against η for variation of Ec for $n = 0.746$

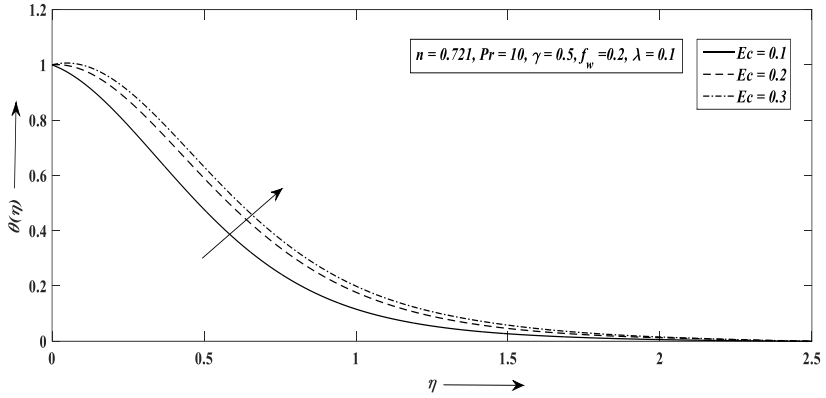

Table 4.2. Values of local skin friction coefficient $Cf_x Re_x^{\frac{1}{n+1}}/2$

f_w	λ	$n = 0.699$	$n = 0.721$	$n = 0.746$
0.2	0.1	0.4236	0.4240	0.4389
0.5	0.1	0.4742	0.5013	0.5091
1.0	0.1	0.6097	0.6322	0.6525
0.2	0.0	0.4395	0.4441	0.4573
0.2	0.5	0.2722	0.3344	0.3381
0.2	1.0	0.2082	0.2254	0.2243

Table 4.3 Values of local Nusselt number $NU_x/Re_x^{\frac{1}{n+1}}$

f_w	λ	γ	Pr	Ec	$n = 0.699$	$n = 0.721$	$n = 0.746$
0.2	0.1	0.5	10	0.1	1.2176	1.0380	0.7454
0.5	0.1	0.5	10	0.1	2.8696	2.6589	2.6071
1.0	0.1	0.5	10	0.1	5.6346	5.5824	5.5209
0.2	0.0	0.5	10	0.1	1.0629	1.0021	0.8198
0.2	0.5	0.5	10	0.1	-0.6598	0.3265	0.4191
0.2	1.0	0.5	10	0.1	-1.4008	-0.2535	0.2515
0.2	0.1	0.2	10	0.1	2.0106	2.0002	1.9286
0.2	0.1	0.6	10	0.1	0.4234	0.3630	0.2351
0.2	0.1	0.7	10	0.1	-0.5795	-0.4674	-0.4833
0.2	0.1	0.5	20	0.1	1.2176	1.0380	0.7454
0.2	0.1	0.5	30	0.1	3.0822	2.9384	2.6481
0.2	0.1	0.5	50	0.1	4.8759	4.8356	4.6682
0.2	0.1	0.5	10	0.0	1.3071	1.1255	1.0897
0.2	0.1	0.5	10	0.2	0.8431	0.6068	0.5305
0.2	0.1	0.5	10	0.3	0.6127	0.3792	0.1797

5. Conclusion

The following conclusion can be drawn from this work:

- The growth of flow index parameters reduces the fluid motion whereas temperature of the fluid enhances with increasing flow index parameter.
- Suction reduces fluid velocity, demonstrating how it helps to control the development of boundary layer.
- Greater suction causes the plate to cool more quickly, which is crucial in many engineering applications, as the temperature of the fluid decreases as the suction parameter increases.
- As the slip parameter rises, the dimensionless velocity diminishes at the surface but grows at greater distances, while the temperature around the boundary layer area enhances.
- The impact of heat generation parameter causes the entire boundary layer's temperature to rise when $\gamma > 0$.
- The dimensionless temperature decreases with increasing Pr. Physically, increasing Pr, produces a reduction in the thickness of the thermal boundary layer for three distinct flow index parameter values.
- It is evident that as Ec rises, the dimensionless temperature rises as well. The reason for this is that decreasing the Eckert number cools the wall, which subsequently conducts heat to the fluid and raises its temperature.
- The local skin-friction coefficient is increased by raising the values of the suction parameter f_w while it is decreased by greater values of the slip parameter λ.
- The growth of the Prandtl number and the suction parameter raises the local Nusselt number, whereas the growth of the slip parameter, heat generation parameter, and Eckert number lowers it.

6. Scope for future work

- There is ample scope to extend this work for further research due to diversified applications in engineering and food sciences.
- Non-Newtonian fluid flows of different fruit and vegetable products can also be studied with the help of same fluid model.
- Fluid flow problems of different geometry can also be considered as per requirement of the food industry.
- Some fluid properties have been discussed in this study but there are many rheological properties of fluids of engineering interest which may be incorporated for further research.
- Flow visualization of the problem may give the clear picture of the obtained results.

References

1. Diamante, L.; aUmemoto, M. Rheological properties of Fruits and Vegetables: A Review. International Journal of Food Properties 2015, 18, 1191-1210.
2. Abdulagatov, A.; Magerramov, M.; Abdulagatov, I.; Azizov, N. Effect of temperature, pressure and concentration on the viscosity of fruit juice: Experimental and modeling. In: *Progress in Food Engineering Research and Development*; Cantor, J.; Ed.; Nova Science Publishers, Inc.: New York, 2008; 61–130.
3. Falguera, V.; Vélez-Ruiz, J.; Alins, V.; Ibarz, A. Rheological behaviour of concentrated mandarin juice at low temperatures. International Journal of Food Science and Technology **2010**, *45* (10), 2194–2200.

4. Vandresen, S.; Quadri, M.; Souza, J.; Hotza, D. Temperature effect on the rheological behavior of carrot juices. Journal of Food Engineering **2009**, *92* (3), 269–274.
5. Vitali, A.A.; Roa, M.A. Flow properties of low-pulp concentrated orange juice: Effect of temperature and concentration. Journal of Food Science **1984**, *49* (3), 882–888.
6. Mahmoud M.A.A., Slip velocity effect on a non-Newtonian power law fluid over a moving permeable surface with heat generation **2011**, Mathematical and Computer Modelling, 54, 1228-1237
7. Ibarz, A.; Gonzalez, C.; Esplugas, S. Rheology of clarified passion fruit juices. Fruit Processing **1996**, *6*, 330–333.
8. Chin, N.; Chan, S.; Yusof, Y.; Chuah, T.; Talib, R. Modelling of rheological behaviour of pummelo juice concentrates using master-curve. Journal of Food Engineering **2009**, *93* (2), 134–140.
9. Goula, A.; Adamopoulos, K. Rheological models of kiwifruit juice for processing applications. Journal of Food Processing and Technology **2011**, *2*, 106.
10. Augusto, P.; Falguera, V.; Cristianini, M.; Ibarz, A. Rheological behavior of tomato juice: steady-state shear and timedependent modeling. Food and Bioprocess Technology **2012**, *5* (5), 1715–1723.
11. Acrious, A., Shah, M.J., Peterson E.E., "Momentum and heat transfer in laminar boundary layer flow on non-newtonian fluids past external surfaces", AIChE Journal. vol. 6, pp: 312–316, 1960.
12. Schowalter, W.R., "The application of boundary layer theory to power law pseudo plastic fluids: similar solutions", AIChE Journal. vol. 6(1), pp: 24-28, 1960.
13. Lee, S.Y., Ames, W.F., "Similar solutions for non-Newtonian fluids", AIChE Journal. vol. 12, pp: 700–708, 1960.
14. Andersson, H.I., Bech, K.H. and Dandapat, B.S., "Magnetohydrodynamic flow of a power law fluid over a stretching sheet", International Journal of Non-Linear Mechanics. vol. 72, pp: 929–936, 1992.
15. Saritha, K., Rajasekhar, M.N. and Reddy, B.S. "Combined effects of soret and dufour on mhd flow of a Power-law fluid over flat plate in slip flow regime", International Journal of Applied Mechanics and Engineering. vol. 23(3), pp: 689-705, 2018
16. Schlichting, H., (1968), Boundary Layer theory, 6th edition, McGraw-Hill, New York.
17. Srivastava, A. C., (1967), Constitutive equation in fluid dynamics, J. Math. Phy. Sc., 2, 345.
18. Wilkinson, W.L.; Non-Newtonian Fluids, Pergaman, Press, 1960.